

## **A simple controller for the nonlinear model of quadrotor helicopters and its application to vision-based landing**

\*Ilan Zohar<sup>1)</sup>, Amit Ailon<sup>2)</sup> and Hugo Guterman<sup>3)</sup>

<sup>1), 2), 3)</sup> *Department of Electrical & Computer Engineering,  
Ben Gurion University of the Negev, Beer Sheva, Israel*

<sup>1)</sup> [ilanzoh@ee.bgu.ac.il](mailto:ilanzoh@ee.bgu.ac.il)

### **ABSTRACT**

This paper considers basic control problems in the model of a quadrotor-type helicopter. Using structural properties of the quadrotor analytical model we preset controllers for stabilizing the attitude and attitude/ altitude subsystems. Although the underlying system is highly nonlinear, the proposed controllers for the relevant tasks are relatively simple and, to a certain extent resemble the structure of PD-type controllers. In order to compensate drift in the quadrotor location (resulting from the nonlinear coupling between attitude and position) a two-mode control strategy has been implemented. Simulation results demonstrate the performance of the proposed controllers. A vision-based controller has been implemented in a small-scale quadrotor for autonomous indoor flight and for precise automated landing using the proposed control strategy.

**Keywords:** Quadrotor; nonlinear model; attitude/altitude; stabilizing controllers; hovering; two-mode controller; vision control

### **1. INTRODUCTION**

Flying objects have always been a fascinating topic for scientists from various disciplines, encouraging all kinds of research and development. The broad field of applications spans both the military and civilian markets. The ability to execute unmanned missions such, as patrol and surveillance, rescue and tracking moving targets, makes the technological framework of flying objects a scientific challenge with many practical implications.

Unmanned vertical take-off and landing system design requires the development and implementation of complex algorithms to control the nonlinear mechanical system. Among this kind of autonomous aerial vehicle, the quadrotor-type helicopter is very attractive for research and examination. Some relevant studies of this system are (Castillo 2004, Castillo 2005, Das 2009, Huang 2009, Michael 2009). For the sake of illustration, Fig. 1 presents a quadrotor in flight.

Although the quadrotor is actuated by four motors, it is an underactuated dynamic system. Unlike the regular helicopters that have variable pitch angle rotors, the quadrotor-type helicopter has four fixed-pitch angle rotors. The quadrotor's motion is generated by varying the rotor speeds thereby changing the aircraft lift force and



Fig. 1 The md4-200 quadrotor helicopter of microdrones equipped with Galaxy S3 during flight

attitude. The quadrotor tilts toward the direction of the slow spinning rotor, which enables acceleration along the selected direction. The spinning directions of the rotors are set to balance the moments and to eliminate the need for a tail rotor. This principle is also used to produce the desired yaw motions. A good controller should properly arrange the speed of each rotor so that the desired states change as required.

The state-of-the-art in quadrotor control technology has drastically changed during the last few years (Kendoul 2007), and the number of projects tackling related problems has considerably increased. Most of these projects are based on commercially available devices like the draganflyer (draganfly), which have since been modified to have more sensory and communication capabilities. The work of (Bouabdallah 2004), for example, has considered simultaneously design and control for quadrotors.

This study is concerned with problem of the basic control problems of the underlying autonomous system. In the first stage of this study, we shall present a simple new controller for regulating the attitude/altitude quadrotor dynamics. The underlying approach is based on the particular structural properties of the system under consideration, whose model is obtained by means of Lagrange formalism. Also, the system under consideration is highly nonlinear and the obtained controller (although nonlinear) is simple to realization and, in fact, resembles a PD-type controller.

The coupling between attitude and position makes the trajectory tracking control problem difficult. However, at least in the case of set-point control, it is possible to adopt a two-mode control scheme as follows. Firstly, a nonlinear controller is applied in order to achieve attitude/altitude regulation, and then, a fine linear control strategy is applied in order to achieve smooth motion towards the desired position coordinates. In the first stage of the current study, we present an analytical approach that leads to an efficient control strategy for trajectory tracking. Next, the proposed control scheme performance is evaluated numerically. Finally, following the analytical study, a vision-based controller has been designed and implemented for demonstrating the automated landing of a small-scale quadrotor in an indoor environment.

## 2. MODELING

The evolution of the system configuration in space can be described by the motion of the center of mass motion and by the motion about the center of mass. Let  $F$  be the total force and  $M$  be the sum of torques applied to the body. The mechanical system motion is governed by the equations.

$$m \frac{dv}{dt} = F$$

$$\frac{dL}{dt} = M, \quad (1)$$

where  $v$  is the velocity of the mass center relative to the inertial frame  $\{x, y, z\}_i$ ,  $L$  is the angular momentum and  $m$  is the total mass of the rigid body.

Let the body coordinate system be attached to the quadrotor as in Fig. 2.

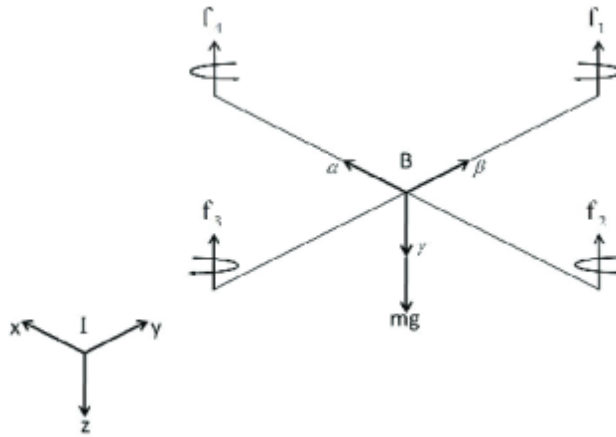


Fig. 2 The quadrotor body frame  $\{ \}_b$ , the inertial frame  $\{ \}_i$ , and the motor thrust forces

Recall that the inertial coordinate system is designated by  $\{x, y, z\}_i$  and the body coordinate system, fixed in the body at the center of gravity is,  $\{\alpha, \beta, \gamma\}_b$ , with unit vectors  $i_b, j_b, k_b$  we have

$$\frac{dv_b}{dt} = \dot{v}_\alpha i_b + \dot{v}_\beta j_b + \dot{v}_\gamma k_b + \omega_b \times v_b$$

$$\frac{dL_b}{dt} = \dot{L}_\alpha i_b + \dot{L}_\beta j_b + \dot{L}_\gamma k_b + \omega_b \times L_b \quad (2)$$

And, in terms of the body frame, (1) is given by

$$m\dot{v}_b + \omega_b \times mv_b = F_b$$

$$J\dot{\omega}_b + \omega_b \times J\omega_b = M_b, \quad (3)$$

where  $J$  is the inertia tensor with respect to the body frame.

The above equations describe how the forces and moments affect the translational and rotational velocity of the rigid body. We should, however, also develop the

kinematic equations. This will allow us to relate quantities in the inertial system in terms of the body coordinate system and vice versa. To start with we, wish to obtain the coordinates of the motion path relative to the inertial frame. We first apply a sequence of rotations using Euler angles  $\{\psi, \theta, \phi\}$ . Initially, the vehicle coordinates coincide with the inertial frame coordinates. We made the following sequence of rotations: 1) a rotation  $\psi$  about the axis  $o\gamma$  car transferring rying the body axes to  $\{\alpha_1, \beta_1, \gamma_1\}$ . 2) A rotation  $\theta$  about  $o\beta_1$  carrying the system  $\{\alpha_1, \beta_1, \gamma_1\}$  to  $\{\alpha_2, \beta_2, \gamma_2\}$  and 3) a rotation about the  $o\alpha_2$  carrying the system  $\{\alpha_2, \beta_2, \gamma_2\}$  to the body frame  $\{\alpha, \beta, \gamma\}_b$ .

The aircraft velocity in terms of the inertial coordinate system is given by

$$v_i = \dot{x}i + \dot{y}j + \dot{z}k \quad (4)$$

and, by using Euler angles  $\{\psi, \theta, \phi\}$  and the associated sequence of rotations (for further details see, e.g., (Etkin 1982)), we have  $v_i = R_i^b v_b$ , where  $R_i^b$  is the rotation matrix from the coordinates  $\{ \}_b$  to the coordinates of  $\{ \}_i$ , that is

$$\begin{bmatrix} \dot{x} \\ \dot{y} \\ \dot{z} \end{bmatrix}_i = R_i^b \begin{bmatrix} v_\alpha \\ v_\beta \\ v_\gamma \end{bmatrix}_b \quad (5)$$

and

$$R_i^b = \begin{bmatrix} c_\theta c_\psi & c_\psi s_\theta s_\phi - c_\phi s_\psi & c_\psi s_\theta c_\phi + s_\phi s_\psi \\ c_\theta s_\psi & c_\phi c_\psi + s_\theta s_\phi s_\psi & -s_\phi c_\psi + s_\theta c_\phi s_\psi \\ -s_\theta & c_\theta s_\phi & c_\theta c_\phi \end{bmatrix}, \quad (6)$$

where  $s_a \equiv \sin a$  and  $c_a \equiv \cos a$ .

*Remark.* Note that the sequence through which Euler rotations have been carried out is not always the same in the relevant references. In fact, to date no standard sequence has been agreed upon. Here we, adhere to the sequence of rotations presented in (Etkin 1982, Section 4.5).

Let the Euler angles vector be  $\xi \equiv [\phi, \theta, \psi]^T$ . We wish to express the relationship between the body angular velocity  $\omega_b$  and the Euler vector rate of change  $\dot{\xi} = [\dot{\phi}, \dot{\theta}, \dot{\psi}]^T$ . Assuming that  $\theta \in (-\pi/2, \pi/2)$ , we have

$$\dot{\xi} = L_{ib}(\xi) \omega_b, \quad (7)$$

where

$$L_{ib} = \begin{bmatrix} 1 & \sin \phi \tan \theta & \cos \phi \tan \theta \\ 0 & \cos \phi & -\sin \phi \\ 0 & \sin \phi \sec \theta & \cos \phi \sec \theta \end{bmatrix} \quad (8)$$

and  $\det L_{ib} = 1/\cos \theta$ . Note that the matrix  $L$  is not a rotation matrix, in general,  $L_{ib} \neq L_{ib}^T$ .

Recalling that  $\xi = [\phi, \theta, \psi]^T$  the equations of motion of the aerial vehicle are given (using (3) and (7)) by

$$\begin{aligned} \dot{v}_b &= -\omega_b \times v_b + F_b / m \\ \dot{\xi} &= L(\xi)\omega_b \\ \dot{\omega}_b &= -J^{-1}\omega_b \times J\omega_b + J^{-1}M_b. \end{aligned} \quad (9)$$

Since the considered rigid body is a flying object, the force  $F_b$  and the moment  $M_b$  are due to the action of the aerodynamic, propulsive, and gravitational field forces. In the current analysis we neglect the aerodynamic generalized forces.

In what follows the, cross product for  $a, b \in R^3$  is expressed as a matrix operator, that is  $S(c)d = c \times d = -d \times c$  where  $S(\cdot)$  is a  $3 \times 3$  skew-symmetric matrix. Applying the rotation matrix  $R_i^b$  in (6), we arrive at the following state-space model for the considered system

$$\begin{aligned} \dot{\chi}_1 &= \chi_2 \\ \dot{\chi}_2 &= R_i^b(\xi)F_b / m + e_3g \\ \dot{\xi} &= L_{ib}(\xi)\omega_b \\ \dot{\omega}_b &= J^{-1}S(J\omega_b)\omega_b + J^{-1}M_b, \end{aligned} \quad (10)$$

where  $\chi_1 = [x_1, y_1, z_1]^T \in [x, y, z]^T$  is the position vector of the vehicle center of mass in terms of the inertial frame,  $\chi_2 = [x_2, y_2, z_2]^T \in [\dot{x}, \dot{y}, \dot{z}]^T$ ,  $e_3 = [0, 0, 1]^T$ ,  $\xi = [\phi, \theta, \psi]^T$  and  $g$  is the gravity constant.

The thrust produced by the  $i$ -th motor is given by (Bouabdallah 2004) as  $T_i = b\Omega_i^2$  where  $b > 0$  is the thrust factor and  $\Omega_i$  is the angular velocity of the rotor. The force and torque vectors in (10) are given by (note that the vector  $F_b$  acts in the negative direction of the  $z_b$  axis in Fig. 2)

$$\begin{aligned} M_b &= \left[ lb(\Omega_1^2 - \Omega_3^2), lb(\Omega_4^2 - \Omega_2^2), \right. \\ &\quad \left. d(\Omega_1^2 + \Omega_3^2 - \Omega_2^2 - \Omega_4^2) \right]^T \\ F_b &= [0, 0, -u]; u = b_{i-1}\Omega_i^2 > 0, \end{aligned} \quad (11)$$

where  $l$  is the distance from the motor to the body center of mass and  $d$  is the drag

factor. The last equation can be represented by the following matrix equation

$$\begin{aligned} [u, M_b^T]^T &= H [\Omega_1^2, \Omega_2^2, \Omega_3^2, \Omega_4^2]^T \\ H &= \begin{bmatrix} b & b & b & b \\ lb & 0 & -lb & 0 \\ 0 & -lb & 0 & lb \\ d & -d & d & -d \end{bmatrix}, \end{aligned} \quad (12)$$

where  $H$  is a nonsingular matrix (in fact  $\det H = 8b^3 dl^2$ ).

Observing (11) and (6), the following representation of (10) will be useful later.

$$\begin{aligned} \dot{\chi}_1 &= \chi_2 \\ \dot{\chi}_2 &= \begin{bmatrix} -c_\psi s_\theta c_\phi - s_\phi s_\psi \\ s_\phi c_\psi - s_\theta c_\phi s_\psi \\ -c_\theta c_\phi \end{bmatrix} u / m + \begin{bmatrix} 0 \\ 0 \\ g \end{bmatrix} \\ \dot{\xi} &= L_{ib}(\xi) \omega_b \\ \dot{\omega}_b &= J^{-1} S(J \omega_b) \omega_b + J^{-1} M_b. \end{aligned} \quad (13)$$

### 3. STABILIZING CONTROLLER FOR THE ATTITUDE/ALTITUDE SUBSYSTEM

#### 3.1 ATTITUDE REGULATION

In the controller design we assume that all state variables are measured. It is important to note that both the  $\xi$ - and  $\omega_b$ -subsystems in (10) are independent of the position and velocity vectors  $\chi_1, \chi_2$ , respectively, while the latter vectors are highly coupled with the attitude vector  $\xi$ .

We concentrate now on the attitude subsystem, namely, the equations

$$\begin{aligned} \dot{\xi} &= L_{ib}(\xi) \omega_b \\ \dot{\omega}_b &= J^{-1} S(J \omega_b) \omega_b + J^{-1} M_b, \end{aligned} \quad (14)$$

Following the approach and results in (Ailon 2004), one obtains the following simple result for attitude regulation.

*Lemma 1.* Consider (14) and let the applied torque be

$$M_b = -\left(L_{ib}^T(\xi)K\xi + B\omega_b\right) \quad (15)$$

where  $K = K^T, B = B^T > 0$  are arbitrarily selected constant matrices. Then, the trivial solution of (10) is locally asymptotically stable.

*Proof.* Consider the Lyapunov candidate function

$$V_a(\xi, \omega_b) = \frac{1}{2} \left[ \xi^T K \xi + \omega_b^T J \omega_b \right], \quad (16)$$

where  $K = K^T > 0$ . Using (15) and substituting  $M_b$  into (10), the derivative of  $V_a$  along the trajectories of the resulting closed-loop system (10), namely,  $\dot{V}_a = \xi^T K \dot{\xi} + \omega_b^T J \dot{\omega}_b$  satisfies

$$\begin{aligned} \dot{V}_a &= \xi^T K L_{ib}(\xi) \omega_b + \omega_b^T S(J\omega_b) \omega_b \\ &\quad - \omega_b^T L_{ib}^T(\xi) K \xi - \omega_b^T B \omega_b \\ &= -\omega_b^T B \omega_b \leq 0. \end{aligned} \quad (17)$$

The second equality follows from the facts that the matrix  $S(J\omega_b)$  is skew symmetric and hence  $\omega_b^T S(J\omega_b) \omega_b = 0$ , and that  $\xi^T K L_{ib}(\xi) \omega_b = \omega_b^T L_{ib}^T(\xi) K \xi$ . Invoking the *LaSalle's invariance principle* (Khalil 2002) the lemma follows. ♦

*Remark:* (i)- The stability property is local since  $L_{ib}(\xi)$  is defined only for  $\theta \in (-\pi/2, \pi/2)$ . Note that the controller in (15) is independent of the system parameters and it is quite similar to a PD controller. (ii)- The controller (15) is independent of the system's physical parameters ( $m$ , and  $J$ ).

### 3.2 ATTITUDE/ALTITUDE REGULATION

Observing the matrix  $R_i^b$  in (6) and the vector  $F_b$  in (11), the attitude/altitude subsystem can be written as

$$\begin{aligned} \dot{z}_1 &= z_2 \\ \dot{z}_2 &= -u \cos \theta \cos \phi / m + g \\ \dot{\xi} &= L_{ib}(\xi) \omega_b \\ \dot{\omega}_b &= J^{-1} S(J\omega_b) \omega_b + J^{-1} M_b. \end{aligned} \quad (18)$$

The control objective is to stabilize (locally) the trivial solution of the system (18) with the state  $\varphi = [z_1, z_2, \xi^T, \omega_b^T]^T \in R^8$  while keeping  $u > 0$  (see (11)). (Without loss of generality we take  $z_{1d} = 0$  as the height at the equilibrium point.)

*Lemma 2.* Consider the system (18) and let the applied torque  $M_b$  be as in (15) and  $u$  be

$$u = m \frac{[g + \alpha z_1 + \beta z_2]}{[\cos \theta \cos \phi]} \quad (19)$$

for arbitrary selected constants  $\alpha, \beta > 0$ . Then, the trivial solution of the resulting closed-loop system is (locally) asymptotically stable and, provided the initial state is in a sufficiently small ball of the origin,  $u(t) > 0$  for all  $t \geq 0$ .

*Proof.* Applying the feedback (19) in the second equation of (18) the, first two equations reduce to the linear subsystem

$$\begin{aligned} \dot{z}_1 &= z_2 \\ \dot{z}_2 &= -\alpha z_1 - \beta z_2. \end{aligned} \quad (20)$$

Clearly, the system (20) is asymptotically stable for any pair  $\alpha, \beta > 0$ . The proof of the lemma is accomplished by recalling Lemma 1 and noting that, provided the initial state of (18) is sufficiently close to the origin,  $\theta(t), \phi(t) \in (-\pi/2, \pi/2)$  and  $u(t) > 0$  in (19) for all  $t \geq 0$ . ♦

In a later stage of this study we shall consider model linearization and thus it is worth noting now that a possible *Lyapunov function* for (20) is  $V_z = Z^T Q Z / 2$  where  $Z = [z_1, z_2]^T$  and  $Q = Q^T > 0$  satisfies the equation

$$QA + A^T Q = -I_2. \quad (21)$$

$I_2$  is the  $2 \times 2$  identity matrix and  $A$  is the system matrix, that is  $\dot{Z} = AZ$  and the derivative of  $V_z$  along the solution of (20) is

$$\dot{V}_z = -Z^T Z. \quad (22)$$

#### 4. A TWO-MODE CONTROLLER

Due to the nonlinear coupling between the attitude and the position variables, the process of attitude/altitude regulation is associated with drift in the  $\{x, y\}$  coordinates. To reduce the resulting drift, we propose a two-mode control scheme as follows: firstly, using the controllers (15) and (19) attitude/altitude regulation is obtained, and then a drift compensation procedure takes place.

The first action of the two-mode control is based on the nonlinear controller  $U = [u, M_b^T]^T$  where  $M_b$  is given by (15) and  $u$  by (19). The second mode which, ensures smooth motion back to the desired position coordinates while keeping the attitude/altitude state in almost the desired position is, based on system linearization. System linearization techniques for quadrotor control appear quite often in the relevant literature; two examples are (How 2008) and (Michael 2010). However, here we consider a different approach that allows us to present properties of the obtained linear model that are useful for designing the second controller mode.

To this end, consider the quadrotor model in (13) with the matrix  $L_{ib}(\xi)$  in (8). In the trivial solution of the subsystem (18)  $M_b = 0$  and (since then  $\theta = \phi = 0$ )  $u = mg$ . Let us take  $u = mg - mu_1$  with  $u_1 = 0$  in the equilibrium point of (18). For this representation of  $u$ , Eq. (13) becomes

$$\begin{aligned} \dot{\chi}_1 &= \chi_2 \\ \dot{\chi}_2 &= \begin{bmatrix} -g c_\psi s_\theta c_\phi - g s_\phi s_\psi \\ g s_\phi c_\psi - g s_\theta c_\phi s_\psi \\ -g c_\theta c_\phi + g \end{bmatrix} \\ &\quad - \begin{bmatrix} -c_\psi s_\theta c_\phi - s_\phi s_\psi \\ s_\phi c_\psi - s_\theta c_\phi s_\psi \\ -c_\theta c_\phi \end{bmatrix} u_1 \\ \dot{\xi} &= L_{ib}(\xi) \omega_b \\ \dot{\omega}_b &= J^{-1} S(J \omega_b) \omega_b + J^{-1} M_b. \end{aligned} \tag{23}$$

Eq. (23) is now written as  $\dot{\zeta} = f(\zeta, \mu)$  where,  $\zeta = [\chi_1^T, \chi_2^T, \xi^T, \omega_b^T]^T$  is the state vector and  $\mu = [u_1, M_b^T]^T$  is the input. We have  $f(0,0) = 0$ . We are considering designing a state feedback control law  $\mu = \gamma(\zeta)$  that stabilizes the system (23), which is the control objective of the second mode of operation. Linearization of (23) about  $\zeta = 0$  and  $\mu = 0$  results in the linear system

$$\dot{\zeta} = A\zeta + B\mu, \tag{24}$$

where

$$A = \left. \frac{\partial f(\zeta, \mu)}{\partial \zeta} \right|_{\zeta=0, \mu=0}; B = \left. \frac{\partial f(\zeta, \mu)}{\partial \mu} \right|_{\zeta=0, \mu=0}. \tag{25}$$

After some computations (see (8) and (23)) we arrive at the following linear model

$$\begin{aligned}
\dot{\chi}_1 &= \chi_2 \\
\dot{\chi}_2 &= \begin{bmatrix} 0 & -g & 0 \\ g & 0 & 0 \\ 0 & 0 & 0 \end{bmatrix} \xi + \begin{bmatrix} 0 \\ 0 \\ 1 \end{bmatrix} u_1 \\
\dot{\xi}_1 &= \omega_b \\
\dot{\omega}_b &= M_b.
\end{aligned} \tag{26}$$

We note that the linear system (26) with the state  $X = [\chi_1^T, \chi_2^T, \xi_1^T, \omega_b^T]^T \in R^{12}$  and input  $\mu = [u_1, M_b^T]^T \in R^4$  is controllable. In fact, the column blocks that span the column space of the controllability matrix are

$$\left\{ \begin{bmatrix} 0 \\ 0 \\ 0 \\ I_3 \end{bmatrix}, \begin{bmatrix} 0 \\ 0 \\ 0 \\ 0 \end{bmatrix}, \begin{bmatrix} 0 \\ \tilde{I}_3 \\ 0 \\ 0 \end{bmatrix}, \begin{bmatrix} \tilde{I}_3 \\ 0 \\ 0 \\ 0 \end{bmatrix} \right\}, \tag{27}$$

where  $I_3$  is the  $3 \times 3$  identity matrix and  $\tilde{I}_3$  is the  $3 \times 3$  secondary diagonal matrix with entries  $\tilde{i}_{31} = 1$ ,  $\tilde{i}_{22} = g$ ,  $\tilde{i}_{13} = -g^2$  and zeros otherwise. Hence, one can design a state feedback  $\mu = -K\zeta$  (where  $K \in R^{4 \times 12}$  is the gain feedback matrix) such that the resulting closed-loop system (24) (and equivalently (26)) has an asymptotically stable trivial solution. Hence, (18) with  $u = -mu_1$  and  $\mu = [u_1, M_b^T]^T = -K\zeta$  is asymptotically stable.

*Remark.* The controllability property is important because it allows one to tune the controller action in the second mode of operation in such a way that the quadrotor will converge smoothly towards the desired operating point while keeping the attitude and altitude within a small neighborhood of the zero state. (Of course, using the same approach the zero altitude ( $z_d = 0$ ) can be replaced by any other reference altitude  $z_d$ .) However, the following point should be emphasized. The proposed approach validation is guaranteed if the drift in the  $xy$  plane during the first mode of operation is sufficiently small in the sense that once the second control mode is applied, the vehicle initial condition belongs to the region of attraction of the resulting closed-loop system with the applied state-feedback. We assume that the time-constant of the attitude mode is much shorter than the time constant of the system dynamics in the  $xy$  plane. In fact, the acceleration of the aerial vehicle in the  $xy$  plane depends only on the projection along this subspace of the applied forces resulting from the motor actions.

## 5. VISION-BASED SYSTEM

A computer vision system combines both hardware and software to extract the marker position (relative to the quadrotor coordinates), using an Augmented Reality (AR) method (Wagner 2007), from video stream images. In our case the vision system is based on an android smart phone (Samsung galaxy s3) with a QUAD CPU, including a video color camera and a set of triple axis sensors: accelerometer, gyro and magnetometer. The measurements from the sensors are combined together to calculate the orientation of the android, relative to the marker. Bluetooth module installed on the md4-200 enables us to connect to the android and send a control command directly to the drone. The software developed for this task runs directly on the android in Java and C++ using arToolkit (ARToolworks) for the android module. The whole vision system runs in real-time at 30 frames per second. The vision system extracts the target's position and calculates the position of the origin of the target relative to drone, using the IMU data to calculate the orientation. The algorithm for marker detection is based on arToolkit, this tool kit provides the position and orientation of the marker. Experiments show that the accuracy of the position and the orientation is not satisfactory, for that reason we, developed some tools to include a calibration process in order to fix the accuracy of the position. In order to correct the orientation of the camera we implement an IMU on the android using the algorithm of (Mahony 2005). A Kalman filter is then implemented in order to improve the estimation of the speed and position of the marker. All data estimations including data from both IMU's (drones, android), were combined and comprised an input for the two-mode controller. The whole process runs at 200  $Hz$  on the android, the commands are sent to the drone via Bluetooth.

## 6. SIMULATION AND EXPERIMENTAL RESULTS

### 6.1 PLATFORM DETAILS

Fig. 1 shows the md4-200 by microdrones company (microdrones). This platform was equipped with the state of the art sensors and double embedded processors. The navigation and control system is based on a MEMS inertial sensor and a processor board, that hosts the closed-loop stabilization routines. We apply a vision based system to verify experimentally the validity and the efficiency of the proposed control algorithms. The android smart phone is mounted inverted to the bottom of the cross-frame where it has a  $360^\circ$  field of view obstructed only by four vertical carbon-fiber rods that are extended down to the landing gear. The phone enables us to control the drone by vision. The applied two-mode control strategy is as follows: firstly the nonlinear controller minimizes the error between the current attitude and the desired one, and then a linear controller operates, and the quadrotor slides towards the marker and lands smoothly. The position feedback is provided by the camera. The simulation results are obtained based on the data of Table 1 associated with the physical parameters of the quadrotor described above. All units in the table are in the MKS system.

Table 1 The quadrotor physical parameters and controller gains

Variable	Value	Variable	Value
$m$	0.8	$l$	0.27
$J_\alpha$	0.0078	$J_\beta$	0.0080
$J_\gamma$	0.034	$T_s$	$1e-3$
$b$	$2.88 \cdot 10^{-7}$	$d$	$8.64 \cdot 10^{-9}$
$K$	$180I_3$	$B$	$240I_3$
$\alpha$	4	$\beta$	4

## 6.2 SIMULATION RESULTS

This subsection is devoted to demonstrate by simulations the controller capabilities in various flying tasks of the quadrotor whose technical features and physical parameters are presented above.

*Example 1.* In this case, the quadrotor control objective is to stabilize the attitude while maintaining a constant altitude. The considered initial condition is  $\xi(0) = [\pi/6, -\pi/6, 0]^T$  (angles in radians) and the pre-specified altitude is  $h = 10[m]$  above ground, or, in terms of the inertial coordinate system  $z_d = -10[m]$  (recall that in a vertical position the positive direction of the  $z$ -axis points towards the ground). Fig. 3 demonstrates attitude set-point tracking and the quadrotor altitude.

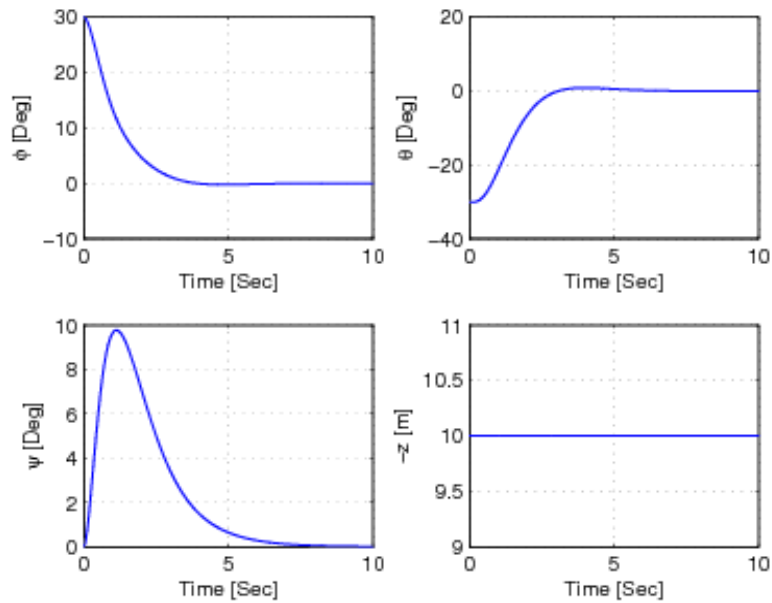


Fig. 3 Time history of the attitude variables while maintaining a constant altitude and regulating the attitude

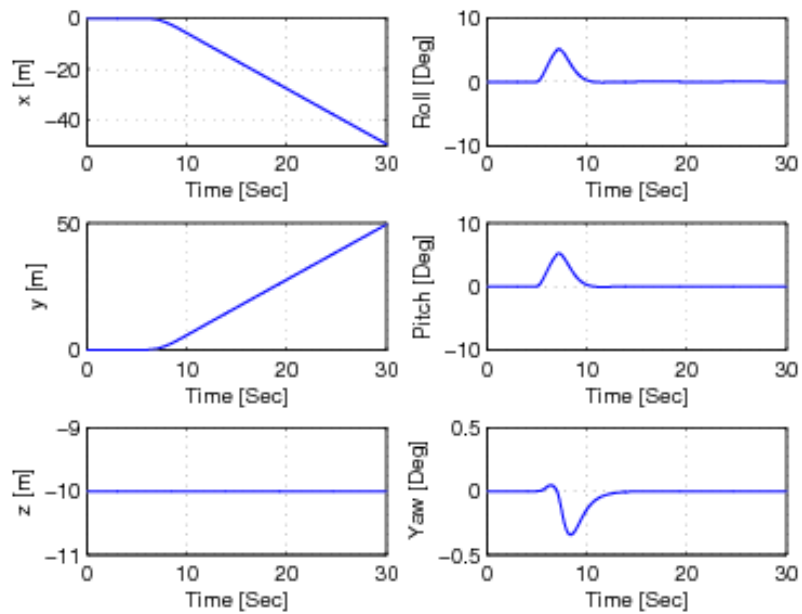


Fig. 4 Drift in the  $\{x, y\}$  coordinates during attitude/altitude regulation

*Example 2.* In this example the effect of the coupling between attitude and position is illustrated. While the controller ensures stabilization of the attitude/altitude subsystem, the quadrotor position changes, as demonstrated in Fig. 4. In this example the initial condition vector is  $[\chi_1^T(0), \chi_2^T(0), \xi^T(0), \omega_b^T(0)]^T = 0$ . At  $t = 5$  [sec.] we implemented a

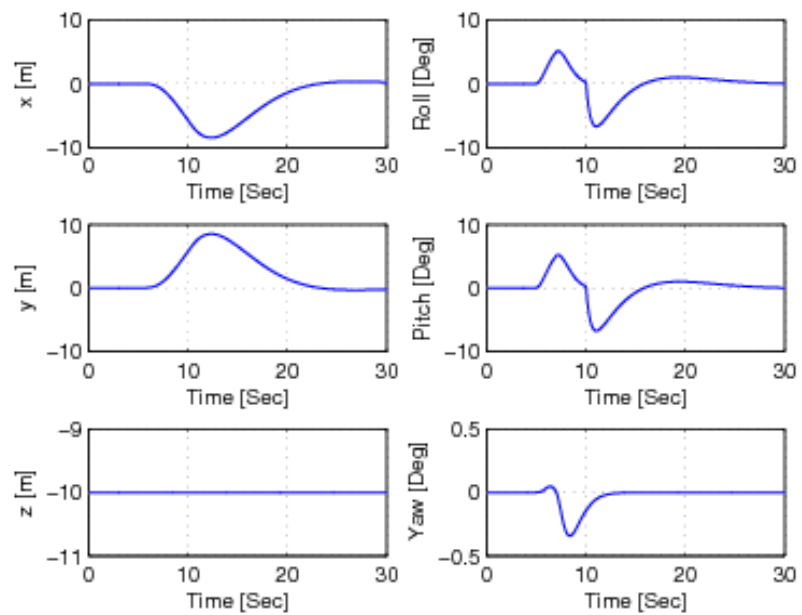


Fig. 5 The action of the second mode controller for correcting drift in the  $\{x, y\}$  coordinates during attitude/altitude regulation

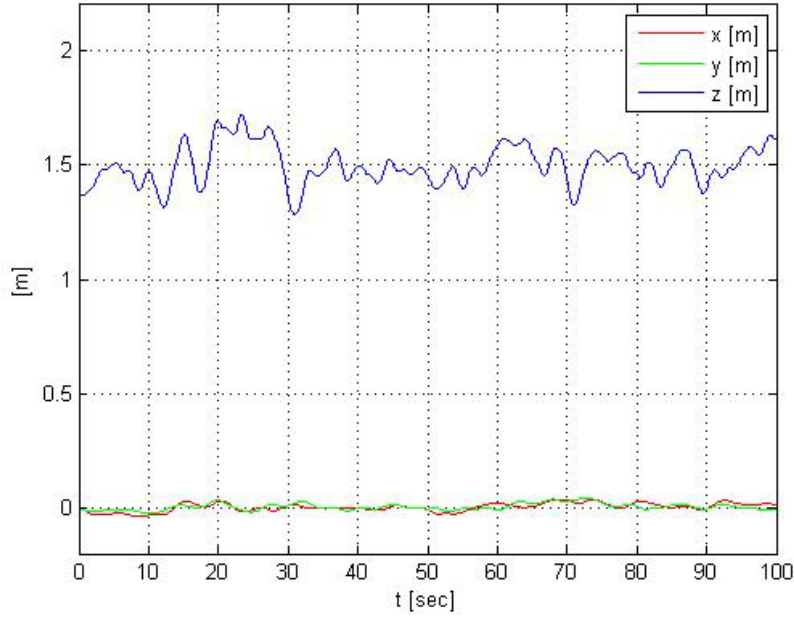


Fig. 6 The quadrotor in a hovering task

constant torque disturbance  $M_b = \text{diag}(2, 2, 0)$  (the torque units are  $[N \cdot m]$ ) during 2 [sec].

*Example 3.* This example demonstrates the action of the two-mode controller. Initially the nonlinear controller is acting for achieving zero attitude at a desired altitude and then the second mode controller is implemented for driving the quadrotor back to the desired  $\{x, y\}$  location. The results are shown in Fig. 5. In this example the initial conditions and the injected disturbance on the applied torque are the same as in Example 2. At  $t = 8$  [sec.], we switched to the second control with  $\mu = [u_1, M_b^T]^T = -K(\zeta - \zeta_d)$  where  $\zeta \in R^{12}$  is the state vector of (26) (or equivalently (24)),  $\zeta_d$  is the desired state vector (with  $\xi_d = 0$ ) and  $K \in R^{4 \times 12}$  is the gain feedback matrix (see the previous section).

### 6.3 APPLYING VISION-BASED FEEDBACK IN INDOOR EXPERIMENTS

This subsection demonstrates the two-mode controller capabilities by means of vision-based marker detection. The quadrotor was commanded to hover. The quadrotor initial attitude is  $\xi(0) = [0, 0, 0]^T$ . The desired height is  $h = 1.5[m]$ , namely,  $z_d = -1.5[m]$ . The objective is to ensure  $\xi(0) \rightarrow 0$  and  $z \rightarrow z_d$ , while keeping the quadrotor above a designated marker. Fig. 6. show the quadrotor during hovering. The standard deviation values of the position error are 1.81 [cm] in x, 1.48 [cm] in y and 8.47 [cm] in z. The

relative high standard deviation, in the z axis is due to the ground effect and low resolution of the barometer sensor.

## 7. CONCLUSIONS

The main goal of this research was to develop nonlinear controllers for stabilizing the quadrotor attitude and altitude configuration during hovering. We have established a relatively simple controller for regulating the attitude/altitude subsystem for the highly nonlinear quadrotor model. Next, the paper proposes a two-mode controller for compensating the drift in the quadrotor location due to the nonlinear coupling between attitude and position. The first mode is based on the attitude/altitude nonlinear controller and in the second mode the proposed controller is based on a linearized model. In constructing the second-mode controller we apply the feedback pole placement technique for achieving smooth convergence towards the desired location while keeping the attitude almost in the zero-state. Simulation results demonstrate the controller potential and performance. Application of the approach in a real system equipped with a vision-based controller for safe landing has been studied and demonstrated in an indoor environment.

## REFERENCES

- Kendoul F., Lara D., Fantoni-Coichot I. and Lozano R., (2007), "Real-time nonlinear embedded control for an autonomous quadrotor helicopter", *AIAA, J. Guidance, Control, Dynam.*, **30**(4),1049-1061.
- Innovative UAV Aircraft & Aerial Video Systems, <http://www.draganfly.com/>.
- Bouabdallah, S., Noth, A. and Siegwart, R. (2004), "PID vs LQ control techniques applied to an indoor micro quadrotor", *IEEE/RSJ International Conference on*, **3**, 2451-2456, September-October.
- Etkin, B. (1982), *Dynamics of Flight Stability and Control*, John Wiley & Sons, New York.
- Ailon, A., Segev, R. and Arogeti, S. (2004), "A simple velocity-free controller for attitude regulation of a spacecraft with delayed feedback", *IEEE Transactions on Automatic Control*, **49**, 125-130.
- Khalil, H. (2002), *Nonlinear Systems*, Prentice Hall, Upper Saddle River, NJ, USA, 3rd Edition.
- Castillo, P., Dzul, A. and Lozano, R. (2004), "Real-time stabilization and tracking of a four-rotor mini rotorcraft", *IEEE Trans. Contr. Syst. Tech.*, **12**, 510-517.
- Castillo, P., Lozano, R. and Dzul, A. (2005), "Stabilization of a mini rotorcraft with four rotors", *IEEE Contr. Syst. Magazine*, **25**, 45-55.
- Das, A., Lewis, F. and Subbarao, K. (2009), "Backstepping approach for controlling a quadrotor using Lagrange form dynamics", *J. Intel. Rob. Syst.*, **56**, 127-151.
- Huang, H., Hoffmann, G.M., Waslander, S.L. and Tomlin, C.J. (2009), "Aerodynamics and control of autonomous quadrotor helicopters in aggressive maneuvering", *Proc. of the IEEE Inter. Conf. Robot. & Autom.*, Kobe, Japan.
- Michael, N. and Kumar, V. (2009), "Planning and control of ensembles of robots with

- non-holonomic constraints”, *Int. J. Rob. Research*, **28**, 962-975.
- How, J.P., Bethke, B., Frank, A., Dale, D. and Vian, J. (2008), “Real-time indoor autonomous vehicle”, *IEEE Contr. Syst. Magazine*, **28**, 51-64.
- Michael, N., Mellinger, D., Lindsay, Q. and Kumar, V. (2010), “The GRASP multiple micro-UAV test bed”, *IEEE Rob. & Autom. Magazine*, **17**, 56-65.
- Microdrones company, [www.microdrones.com](http://www.microdrones.com), Germany.
- Wagner, D. and Schmalstieg, D. (2007), ARToolKitPlus for Pose Tracking on Mobile Devices, *Computer Vision Winter Workshop*.
- ARToolworks, <http://www.artoolworks.com>
- Mahony, R., Hamel, T. and Pflimlin, J.M. (2005), “Complementary filter design on the special orthogonal group  $SO(3)$ ”, *Decision and Control, 2005 and 2005 European Control Conference, CDC-ECC '05, The 44th IEEE Conference on*, 1477-1484, 12-15.